

Prostate Segmentation with Random Walker by Automatic Seed Generation

Nubwimana Rachel¹, Kewen Xia², Mukunde Nshuti Jules³

*School of Electronics and Information Engineering, Hebei University of Technology, Tianjin 300401, China
Received 08 May 2021; Accepted 23 May 2021*

Abstract: Prostate cancer is the second driving reason for a malignant growth in deaths among men. Medical imaging contributes a lot in the therapeutic discipline due to the fact of its wide use in disease analysis and treatment of patients. In this paper, we present the Random Walker algorithm that incorporates the intensity features in prostate MR images and its shape variability to overcome challenges. The RW algorithm was developed for interactive segmentation allow the user to pre-segment small seeds in the foreground and background of the prostate region. From the seeds, the algorithm computation would then carry out the entire segmentation based on graph theories. The segmentation of prostate magnetic resonance imaging is a difficult task. During the test and training, 113 2D slices of prostate MR images from different patients were acquired on a 1.5T, where we used DSC, JC, PREC, and REC as evaluation metrics. The single Atlas-based method was employed to provide prior information without the manual intervention of a trained technician, it was later improved by Multi atlas-based segmentation, the improved Random Walker with Atlas-based segmentation algorithm yielded good results compared to the three other methods.

Keywords: Atlas-based segmentation, Image Segmentation, Magnetic Resonance Imaging segmentation, Random Walker.

Acknowledgment

This work was supported by the National Natural Science Foundation of China (No. U1813222), Tianjin Natural Science Foundation (No. 18JCYBJC16500), and Key Research and Development Project from Hebei Province (No.19210404D).

Nubwimana Rachel¹ is a master student with the Hebei University of Technology with the department of Artificial Information Processing in China Tianjin (Email: rachelsea68@gmail.com).

Prof. Xia Kewen² serves as a professor and PhD candidate supervisor in Hebei University of Technology, China. His research interests mainly cover intelligent information processing, wireless communications, smart antennas, big data mining, oil logging and other fields. (Email: kwxia@hebut.edu.cn).

Mukunde Nshuti Jules³ is a master graduate from Jiaotong University in Computer Science Department (Email: julesmuku@gmail.com).

I. INTRODUCTION

A prostate is an organ male reproductive gland that secretes the fluid to sustain and preserve the sperms. Prostate cancer comes on the list of dangerous cancers causing death increase amongst men these days. As in 2018, the evaluation has shown that 18 million cases were found where 43% of cases are from lung, female breast, and prostate cancers and among them, 9.6 million individuals have lost life worldwide. Human life is in danger if no improvement is made because the projection statistics shows that the cancer cases will increase up to 62% in 2040[1].

Among the cases that appeared in 2019, at least 1.3 million cases were from prostate cancer and this presented 15% of cancer diagnosed in men where 70% of those cases were found in low- and middle-income countries. The World Health Organization (WHO) statistics classify this cancer on the second frequent tumor amongst men and comes in third place with 7,1% of total cases amongst both genders after lung with 11,6% and female breast 11,6% of total cancer cases[2].

Klein et al.[3] followed a multi-atlas approach to segment the prostate. Another way of Probabilistic atlas segmentation was used by Ghose et al.[4] in graph cuts method, where the energy minimization of the posterior probabilities for a voxel which makes a part of the prostate, was obtained by the atlas-based segmentation and a random forest classification.

In another research conducted there are so many other papers about atlas segmentation [4]–[5]–[6]–[7] and [8] Affine registration and subsequently a non-rigid registration using cubic B-spline[9] in a multi-resolution framework was used to register the training volumes to the test volumes. The corresponding transformation was applied to the label images of the training dataset. Recently, Dowling et al.[10] improved on

the results obtained by [11] by introducing a pre-processing step of bias field correction, histogram equalization, and anisotropic diffusion smoothing. Dowling et al. then used rigid, affine, and diffeomorphic demons registration to generate multiple labels of the test image. Most similar labels were identified and fused to generate the final segmentation. Langerak et al.[12] proposed a new schema for the fusion of the labels in a multi-atlas segmentation framework. They proposed to combine the segmentation result of all the labels to produce the gold standard the target label. Each of the labeled images of each of the atlas was compared to the target label. Labels below a certain threshold were discarded and the target label is re-estimated with labels that have already been selected. In 2015 [13] studied the implementation of the Mask-RCNN model to segment the prostate and ILs, The process continues iteratively to provide the final estimated segmentation label [14] and [15].

MRI is a non-intrusive imaging technique that produces detailed information about anatomical images in three dimensions without the use of destructing radiation. accurate result in prostate segmentation from MRI remains to be challenging due to subsequent several reasons such as diffused boundaries due to prostate surroundings its wide variability in shape due to the movement of the patient[16]. In 2018[17] proposed a context classification based, random walk algorithm for prostate segmentation. In 2020 Sijie Wang Proposed (GRPCA) model is based on the nuclear norm, which usually underestimates the singular values of the low-rank matrix[18]. Under these difficult conditions and without having a prior model to constrain the segmentation, most of the previously proposed algorithms are prone to errors. Thus, our research is based on the development of the best approach to delineate the prostate from its surrounding tissues in an accurate way using Random Walker. We used other different approaches, Semi-Automatic segmentation approach, Single atlas-based segmentation method, and Multi-Atlas-based approach.

II. METHODOLOGY

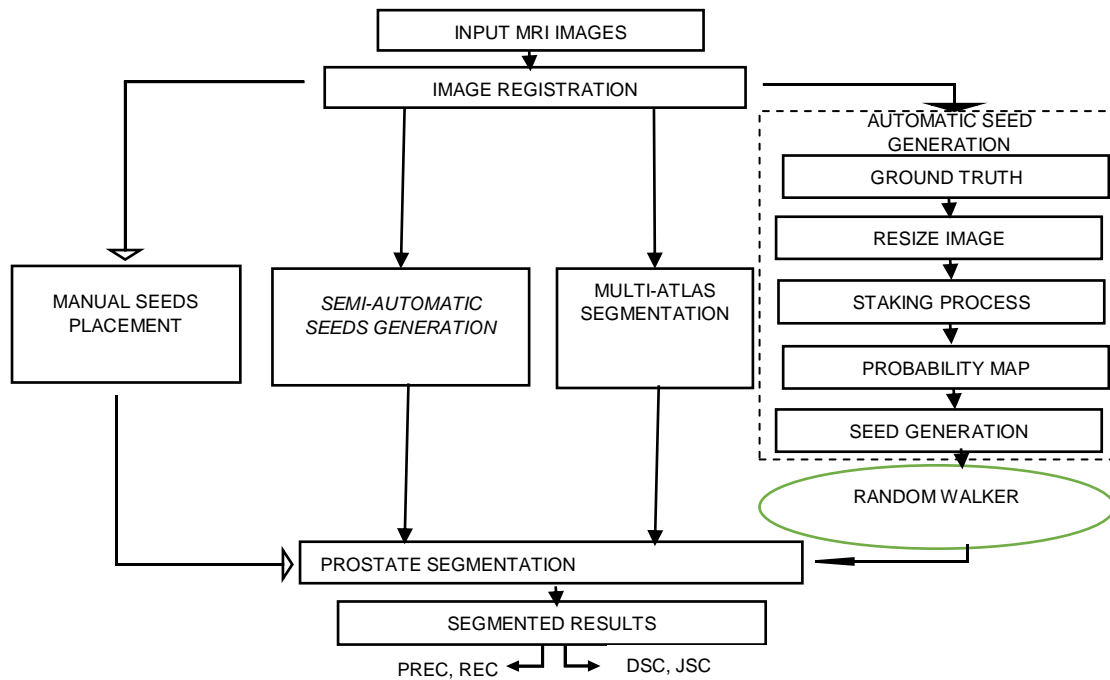


Figure 1: Block diagram summarizing the prostate segmentation with Random Walker.

The various units involved are as follows:

- I. MRI data input.
- II. Data registration of MR prostate images
- III. Seeds generation
- IV. Prostate segmentation
- V. Results evaluation

The algorithm presented in this part depends basically on the Random Walks Segmentation algorithm[19]. A large part of this work was about coding and we used an open-source and highly portable Python programming language, in combination with the scientific libraries Numpy, Scipy, and Opencv. All development and

computations were performed on standard desktop machines. However, while this method shows to be less time consuming by avoiding manual annotation of all pixels, manually positioning the seeds remains a time-consuming process, particularly once a large dataset has to be computed[20].

The proposed research technique is introduced in the following block diagram and a detailed explanation of the whole process will be provided in the next paragraphs.

MRI data input MRI is believed to be an associate imaging modality that depends on the employment of magnetic fields and on radio waves to capture images of different organs and tissues inside the body. We used MRI prostate images to have clear information about the prostate contour which enabled us to segment this organ from its surrounding. We used different modalities of T2W-MRI throughout our work.

Data registration of MR prostate images A crucial issue within the medical imaging field relies on image registration that is of importance in increasing the information we can realize in imaging datasets. Different images taken at totally different times and from numerous viewpoints however from one scene are spatially matched during this process. The main goal of this process is to line up source images with target one, according to feature detection, feature matching, or image transformation.

Seeds generation the Random-walker algorithm requires the user's interaction to initialize the foreground and background seeds manually in the image which saves time. The improvement of this methodology is to come up and label those seeds automatically for quick computation. To do this, we applied the Atlas method. In last, we also explored the use of manual seeds placement, semi-automatic seeds placement, and Multi-Atlas method and we have compared all the results.

Prostate segmentation and results evaluation we used, manual, semi-automatic, and automatic seed generation, the results show that Random Walker with Atlas segmentation is more accurate compared to other methods.

a) Manual Seed Generation Methods

The second part of my algorithm is the use of normal random walks processes of generating the seeds, the prostate close tissues and relative position of the prostate between individuals could be one among the challenges of segmenting the prostate. Therefore, it is of importance to develop a segmentation approach whose prior information is not based on boundary position and the prostate shape, but an approximation of relative prostate's position and its surrounding tissues. To do this, computation of an edge map of our prostate region by computing the local variance of the intensity on a small patch centered on each pixel will be performed. Then, we sampled the seeds on a regular grid, with a high enough density to make sure that the prostate and surrounding tissues contain several seeds.

b) Single Atlas -Based Segmentation

Prostate segmentation in MR images is a challenging task because the intensity distribution inside the prostate gland is characterized by pixel/voxel inhomogeneity. Therefore, accurate prostate segmentation cannot rely on intensity information alone. Few authors have based their methods on intensity information yet incorporated additional knowledge about the general prostate shape in the segmentation. Most studies have used either atlas-based methods, deformable methods, or statistical models as described in the literature of this work.

Atlas-based segmentation is popular to turn the segmentation difficulties into a registration problem. An atlas is created using a training set with manual delineations of the object of interest and then represents the probability for that given label which belongs to the object of interest and registers it to the target image. Recently, Atlas Based has been applied in radiotherapy treatment planning to automate the prostate. In Atlas Based approach, an atlas is constructed by compiling many images of different subjects with corresponding segmentations generated manually by an expert. According to Mallawi Abrar[21], the atlas describes the location, shape, and spatial relationship among anatomical structures by picking out the best atlas candidate image followed by image registration of that atlas subject and target subject images. A single atlas-based segmentation makes use of information from a single expert segmented reference (atlas) image. An extension of this idea is the multi atlas-based segmentation (MAS) technique.

c) Multi-Atlas Segmentation

Multi atlas-based segmentation (MAS) technique was introduced as an improvement over the single atlas-based segmentation technique (SAS). MAS draws from extracting information from similar atlases to make label decisions in an input test image. The basic idea is to assess the majority vote of the reference atlases for a particular voxel. In comparison to SAS, MAS represents information of a wider variety of anatomical variations since label information for a given structure based on multiple reference images is made available. Iglesias et al.[5] reviewed different MAS methods for the procedural steps in performing MAS.

The MAS scheme can be broken into three steps; identification of the most similar reference atlases, comparison of the structure of interest across the references and (label estimation) then label decision-based on the majority. This step of combining label information from multiple atlases is often termed label fusion. The

problem of atlas selection, however, remains unexplored. Current state-of-the-art MAS methods rely on image similarity to select a set of atlases. Unfortunately, this heuristic criterion is not necessarily related to segmentation performance and, thus may undermine segmentation results. To solve this simple but critical problem, we used the Random Walker Algorithm with Atlas-based segmentation.

Random Walker

A random walker is an algorithm for image segmentation. This approach exhibits all of these following qualities Fast computation, Fast editing, and ability to produce an arbitrary segmentation with enough interaction, Intuitive segmentations.

From an image I with N pixels, we built a graph $G=(V, E)$, with representing the set of nodes, $V=N$, and E the set of edges, where the i – th node v_i corresponds to the i – th pixel of image I . We denote the edge connecting the nodes with indices I and j as e_{ij} , and its weight as. Since the graph is undirected, and denote the same edge and their weight is the same: $w_{ij} = w_{ji}$ The set of edges is only composed of pairs of adjacent pixels, such that graph G contains only cliques of order 0 and 1 . We also denote the neighborhood of pixel i as

$$N_i = \{v_j / e_{ij} \in E\}. \tag{1}$$

In our approach, a variety of pixels with known seeds are marked. The probability of the first arrival to those pixels is calculated along the random walk for all labeled pixels. The first labeled seed which has the highest probability of random walk leaving from an unlabeled pixel is labeled with the same label value according to the calculated probabilities.

Probabilistic Explanation

The global label assignment is modeled by a random variable in our method. We denote the probability of assignment of pixel i to label s as $x_i^s = \Pr(l(i) = s)$. We denote the transition probability from node i to node j as p_{ij} . By assuming that I possess a set VM of seeds, i.e. pre-labeled nodes for each label. We denote the set of unknown nodes as V_U such that $V_M \cup V_U = V$ and $V_M \cap V_U = \emptyset$. For convenience in the notations, we denote the sets of indices of the nodes in V_U and V_M as U and M . Since the label of marked pixels is known for probability assignment 1 or 0.

$$\forall i \in M, x_i^s = \begin{cases} 1 & l(i)=s \\ 0 & l(i) \neq s \end{cases} \tag{2}$$

We denote to the probability vector for label s as x^s which contains x_i^s for each pixel. Then, without loss of generality, we can assume the variables in x^s are ordered so that we can write:

$$x^s = \begin{bmatrix} x_U^s \\ x_M^s \end{bmatrix} \tag{3}$$

Where x_U^s x_M^s and are the vectors containing the assignment probabilities for unknown and marked nodes in V_U and V_M . Therefore, the assignment probability of an unknown node $v_i \in V_U$ is expressed for the assignment probability of all the nodes in its neighborhood N_i : $\forall i \in U, x_i^s = \sum_{v_j \in N_j} p_{ij} x_j^s$ (4)

Since all nodes have the same property, the assignment probabilities are all represented at once in matrix form. We denote the transition probability matrix as Π .

$$\Pi = \begin{cases} p_{ij} & \text{if } e_{ij} \in E \\ 0 & \text{otherwise} \end{cases} \tag{5}$$

The transition probabilities are to be set accordingly to the desired properties of the segmentation. Our work is to take a boundary in an image as a result of an intensity pattern where many side-by-side pixels from different intensities form a continuous curve. In our probabilistic framework, this leads to having higher probability transitions for pairs of pixels having various intensities and lower probability transitions for pixels having similar intensities. A well-known choice for transition probability is the Gaussian kernel:

$$w_{ij} = \exp\left(-\beta (I_i - I_j)^2\right) \tag{6}$$

Where w_{ij} is defined as the weight for the edge e_{ij} . Since p_{ij} is a probability, the transition probability will be given by this formula:

$$p_{ij} = \frac{w_{ij}}{\sum_i w_{ij}} \tag{7}$$

By defining A as non-normalized transition matrix:

$$\begin{cases} w_{ij} \text{ if } e_{ij} \in E \\ A_{ij} = 0 \text{ otherwise} \end{cases} \tag{8}$$

Therefore, the Random Walks objective function is defined as:

$$E_{RW}^s(x^s) = \frac{1}{2} (X^{ST} L X^s) \tag{9}$$

Where L is the un-normalized combinatorial Laplacian matrix $L = D - A$ and D as the diagonal matrix.

By decomposing L into sub-blocks for marked and unknown nodes, hence defining sub-blocks L_U , L_M and B as

$$L = \begin{bmatrix} L_U & B \\ B^T & L_M \end{bmatrix} \tag{10}$$

Which allows writing

$$E_{RW}^s(x^s) = \frac{1}{2} \begin{bmatrix} X_U^{ST} \\ X_M^{ST} \end{bmatrix} \begin{bmatrix} L_U & B \\ B^T & L_M \end{bmatrix} \begin{bmatrix} X_U^s \\ X_M^s \end{bmatrix} \tag{11}$$

By differentiating equation (9) for the unknown variables, we obtain:

$$L_U X_U^s = -B X_M^s \tag{12}$$

The variable X_U^s represents the set of probabilities corresponding to unmarked nodes; X_M^s is the set of probabilities corresponding to marked nodes; “1” for foreground nodes and “0” for background nodes.



Figure 2: Graph summarizing how seed will be generated in atlas method.

Random walker prostate segmentation

In this part of our methodology, we selected slices with a visible prostate shape and we generated ground truths to be used for future processes in Atlas registration. During registration, generated ground truth images must have the same pixel size and same image size. This is for critical use during the stacking process which demands those requirements for all images. No-rigid transformations obtained during the registration process were then used to stack together all images representing contours generated manually into one image space. After the stacking process, a probability map was generated in that image space and a certain level was chosen to extract the inner seed (foreground seed) and the outer seed (background seed). These seeds generated in Atlas are those which was considered as automated initialized seeds in the random walks approach.

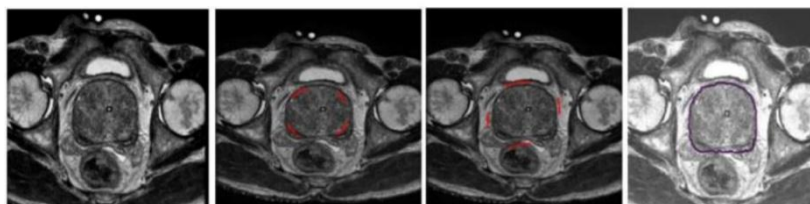


Figure 3: Appearance model for RW in prostate segmentation.

(left) is an original image; In (center) are the foreground and background seeds as red lines; At the (right) is a segmented image.

It was sufficient that they were well placed inside the target region and the Random Walks algorithm would segment the contours accurately. Through a sampling stage, unlabeled seeds were generated within the image domain. Each seed has taken into consideration as a node and accredited to a label. The weight of the edges within the seeds was set to provide information about the existence or non-existence of the outer-line between foreground and background seeds and the similarities between the edges.

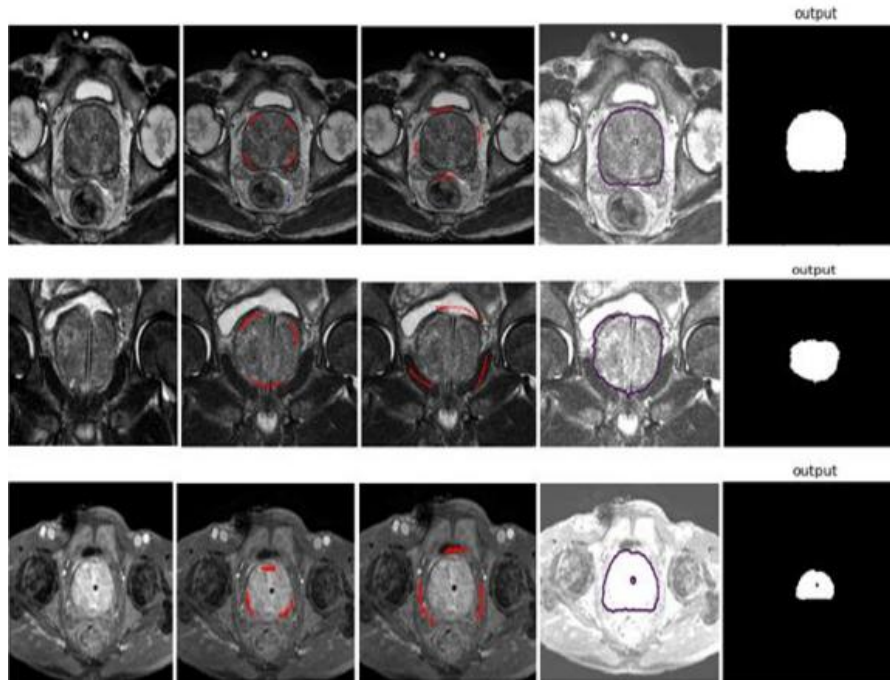


Figure 4: Detailed steps of Random Walker segmentation method.

The above figure shows the results we obtained from input to segmented results (from left to right).

III. RESULTS EVALUATION

The true boundaries of the prostate should be identified to evaluate an image segmentation algorithm, such a process is often referred to as ground truth that has to be created. This section provides details on how the experiment was set up and how their outcomes were evaluated. For evaluation of this method, a comparison between different prostate MRI images and data established ground truth images were made. Then that comparison was further evaluated using the Dice coefficient and Jaccard coefficient, two of the most widely used evaluation metrics in medical imaging.

In automatic seed placement, Atlas registration used ground truths generated from slices with visible prostate shape. Those generated ground truth images must have the same pixel size and same image size. Non-rigid transformations obtained during the registration process was then used to stack together all images representing contours generated manually into one image space. After the stacking process, a probability map was generated in that image space and a certain level was chosen to extract the foreground seed and background seed.

It was sufficient in manual labeling that few seeds were well placed inside the target region and the Random Walks algorithm would segment the contours accurately. Through a sampling stage, unlabeled seeds were generated within the image domain. Each seed has taken into consideration as a node and accredited to a label. The weight of the edges within the seeds was set to provide information on the existence or non-existence of the outer-line between foreground and background seeds and the similarities between the edges. By using the Dice index and Jaccard index together, both overall and detailed performances of the method were evaluated. This explains why one can see this combination often used in the existing literature as the evaluation metric. In general, the better result gives a higher Dice index and a higher Jaccard index.

Evaluation Metrics

We ran both automatic and semi-automatic algorithm on the set of 113 T2W slice images from 113 different patients for which we had delineated their ground truth images as our reference segmentations and for the main purpose of comparison to evaluate our outcome. We compared each segmentation result against the ground truth reference segmentations using five popular metrics DSC and JC, True Positive (TPVF), True Negative (TNVF), and Precision.

Given A as our algorithm results and B as ground truths, the Dice and Jaccard are computed respectively by:

$$DSC = \frac{2 \times |A \cap B|}{|A| + |B|} \quad (13)$$

$$J(A, B) = \frac{|A \cap B|}{|A \cup B|} \quad (14)$$

$$REC = \frac{|A \cap B|}{|B|} \quad (15)$$

$$PREC = \frac{|A \cap B|}{|A|} \quad (16)$$

For the above evaluation metrics used, if the output resulting from our segmentation algorithms were identical to the ground truth from manual segmentation, it would have Dice and Jaccard coefficients close to 1; conversely, if it is entirely different from the ground truth, its Dice and Jaccard coefficients would tend to be 0. So, the more the result looks similar to ground truth, our evaluation index gets close to 1 and more the results look not similar to the ground truth, our evaluation metrics to decrease tending to 0.

Table 1: Summary of performance of different methods

Steps	Methods	DSC	JSC	REC	PREC	Comments/ Observations
1	<i>Semi-Automatic Seeds Generation (ours)</i>	0.72	0.73	0.71	0.70	Semi-Automatic seeds Generation was quiet not what we were expecting. The results were good.
2	<i>Atlas-based Segmentation(ours)</i>	0.93	0.90	0.90	89	Single Atlas-based segmentation is more accurate that Semi-automatic segmentation.
3	<i>Multi-Atlas Segmentation [21]</i>	0.92	0.90	0.91	0.90	Multi-Atlas segmentation is only 1% accurate than single atlas-based Segmentation.
4	<i>Random Walker Segmentation (ours)</i>	0.97	0.98	0.96	0.97	Random Walker was a success compared to other methods.

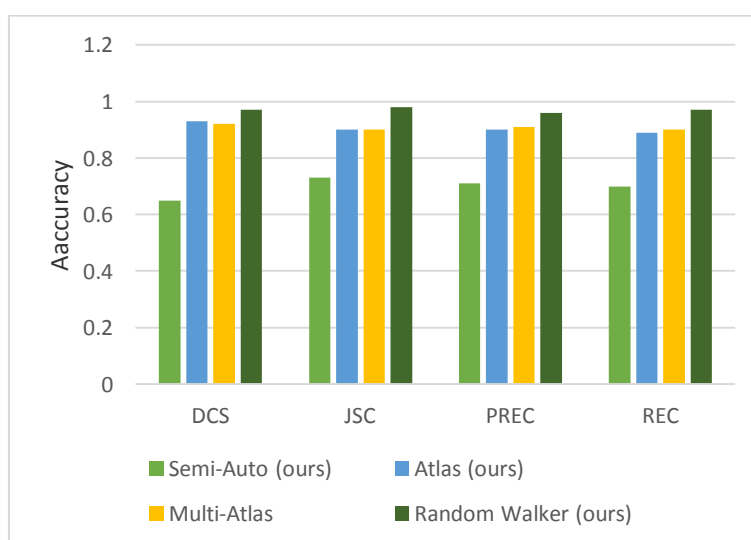


Figure 5: Accuracy comparison.

IV. CONCLUSION

In this paper, we divided the task of seed initialization into automated atlas-based seeds initialization and manual seed initialization for the RW algorithm to segment the prostate. The main idea of this work was to separate the prostate from its surroundings using both strategies and compare the results. The key idea of the approach is based on placing seeds (foreground and background seeds) automatically and manually in the image to get prostate contour.

The second task being to create the ground truth from training images that enable one to compare the similarity between the two sets of images, one set resulting from automatic or manual seed placement and the

other from the ground-truth. Both seeds initialization methods generated good results compared to ground truth, the Random Walker with Atlas segmentation results yielded good results compared to the other methods, which indicates success in the segmentation of the prostate.

The third task was to use Random Walker with Atlas-based segmentation. Although atlas-based methods simplify the segmentation process by making it more automated, such methods are often very sensitive to the computationally expensive image registration step. The experiments conducted show the accuracy and efficiency of our method.

Through Even though the results from both the segmentation method are promising, there is a small difference between SAS, MAS, and Atlas segmentation with Random Walker. We obtained good results comparing Atlas with Random Walker algorithm's segmentation accuracy, as measured by DSC, JC, PREC, and REC, Atlas segmentation with Random Walker is excellent compared to other methods about manual contouring and less time-consuming. The increase in DSC and Jaccard values in an automatic approach means that for future work, we may put more effort into improving the automatic methods since the similarity-error difference between these methods is small compared to the ground truth.

REFERENCES

- [1] F. Bray, J. Ferlay, I. Soerjomataram, R. L. Siegel, L. A. Torre, and A. Jemal, "Global cancer statistics 2018: GLOBOCAN estimates of incidence and mortality worldwide for 36 cancers in 185 countries," *CA. Cancer J. Clin.*, vol. 68, no. 6, pp. 394–424, 2018, doi: 10.3322/caac.21492.
- [2] Z. Khazaei, M. Sohrabivafa, V. Momenabadi, L. Moayed, and E. Goodarzi, "Global cancer statistics 2018: Globocan estimates of incidence and mortality worldwide prostate cancers and their relationship with the human development index," *Adv. Hum. Biol.*, vol. 9, no. 3, p. 245, 2019, doi: 10.4103/2321-8568.262891.
- [3] Z. Tian, L. Liu, and B. Fei, "A fully automatic multi-atlas based segmentation method for prostate MR images," vol. 9413, pp. 1–7, 2015, doi: 10.1117/12.2082229.
- [4] J. Egger, "PCG-Cut: Graph Driven Segmentation of the Prostate Central Gland," *PLoS One*, vol. 8, no. 10, pp. 1–6, 2013, doi: 10.1371/journal.pone.0076645.
- [5] J. E. Iglesias and M. R. Sabuncu, "Multi-atlas segmentation of biomedical images: A survey," *Med. Image Anal.*, vol. 24, no. 1, pp. 205–219, 2015, doi: 10.1016/j.media.2015.06.012.
- [6] Š. Martin, J. Troccaz, and V. Daanen, "Automated segmentation of the prostate in 3D MR images using a probabilistic atlas and a spatially constrained deformable model," *Med. Phys.*, vol. 37, no. 4, pp. 1579–1590, 2010, doi: 10.1118/1.3315367.
- [7] O. D. L. Bornstein M.H., Putnick D.L., Gartstein M.A., Hahn C.S., Auestad N., "Multiatlas Segmentation as Nonparametric Regression.," *Physiol. Behav.*, vol. 176, no. 1, pp. 139–148, 2017, doi: 10.1016/j.physbeh.2017.03.040.
- [8] B. S. ABRAR A. MALLAWI, "Atlas Selection for Automated Segmentation of Pelvic CT for Prostate Radiotherapy," 2015.
- [9] W. Chen *et al.*, "Cancer statistics in China, 2015," 2016.
- [10] Y. Roh, G. Heo, and S. E. Whang, "A Survey on Data Collection for Machine Learning: A Big Data - AI Integration Perspective," *IEEE Trans. Knowl. Data Eng.*, pp. 1–1, 2019, doi: 10.1109/tkde.2019.2946162.
- [11] S. Song, Y. Zheng, and Y. He, "A review of Methods for Bias Correction in Medical Images," *Biomed. Eng. Rev.*, vol. 3, no. 1, pp. 1–10, 2017, doi: 10.18103/bme.v3i1.1550.
- [12] H. Wang and P. A. Yushkevich, "Multi-atlas segmentation with joint label fusion and corrective learning—an open-source implementation," *Front. Neuroinform.*, vol. 7, no. November, pp. 1–12, 2013, doi: 10.3389/fninf.2013.00027.
- [13] Z. Dai *et al.*, "Segmentation of the Prostatic Gland and the Intraprostatic Lesions on Multiparametric MRI Using Mask-RCNN," 2015.
- [14] D. S. Prabha and J. S. Kumar, "Performance evaluation of image segmentation using objective methods," *Indian J. Sci. Technol.*, vol. 9, no. 8, pp. 1–8, 2016, doi: 10.17485/ijst/2016/v9i8/87907.
- [15] N. Kuo, J. Lee, and A. Deguet, "NIH Public Access," no. May 2014, 2010, doi: 10.1117/12.844520.
- [16] S. Ghose *et al.*, "A Survey of Prostate Segmentation Methodologies in Ultrasound , Magnetic Resonance and Computed Tomography Images To cite this version : HAL Id : hal-00695557 A Survey of Prostate Segmentation Methodologies in Ultrasound , Magnetic Resonance and Computed ," 2012.
- [17] R. Guo, Z. Tian, B. Fei, I. Sciences, and C. Science, "HHS Public Access," vol. 44, no. 10, pp. 5128–5142, 2018, doi: 10.1002/mp.12396.A.
- [18] S. Wang, K. Xia, L. Wang, J. Zhang, and H. Yang, "Improved RPCA method via non-convex regularisation for image denoising," *IET Signal Process.*, vol. 14, no. 5, pp. 269–277, 2020, doi: 10.1049/iet-spr.2019.0365.

- [19] L. Grady, "Random walks for image segmentation," *IEEE Trans. Pattern Anal. Mach. Intell.*, vol. 28, no. 11, pp. 1768–1783, 2006, doi: 10.1109/TPAMI.2006.233.
- [20] P. Baudin, "Graph- based segmentation of skeletal striated muscles in NMR images To cite this version : HAL Id : tel-00858584," 2014.
- [21] C. P. G. Machado, "Robust Image Segmentation Applied to Magnetic Resonance and Ultrasound Images of the Prostate," 2012.

Nubwimana Rachel. A, et. al. "Prostate Segmentation with Random Walker by Automatic Seed Generation." *IOSR Journal of Engineering (IOSRJEN)*, 11(05), 2021, pp. 30-38.